Journal of Molecular Catalysis A: Chemical 356 (2012) 29–35

Contents lists available at SciVerse ScienceDirect

Journal of Molecular Catalysis A: Chemical

journal homepage: www.elsevier.com/locate/molcata

Effective Dawson type polyoxometallate catalysts for methanol oxidation

Leila Dermeche[a,b], Nassima Salhi[a], Smain Hocine[a], René Thouvenot[b], Chérifa Rabia[a,*]

[a] Laboratoire de Chimie du Gaz Naturel, Faculté de Chimie, Université des Sciences et de la Technologie Houari Boumediène, USTHB, BP 32, El-Alia, 16111 Bab-Ezzouar, Alger, Algérie

[b] Laboratoire de Chimie Inorganique et Matériaux Moléculaires, Université Pierre et Marie Curie, 4, Place Jussieu, 75252 Paris Cedex 05, France

ARTICLE INFO

Article history:
Received 8 November 2011
Received in revised form
19 December 2011
Accepted 21 December 2011
Available online 2 January 2012

Keywords:
Dawson anions
Methanol oxidation
Dimethyl ether
Formaldehyde
Methyl formate

ABSTRACT

Dawson type polyoxometallates $K_6P_2Mo_xW_{18-x}O_{62}$ (x = 0, 5, 6) and α1 and α2-$K_7P_2Mo_5VW_{12}O_{62}$ were prepared and characterized by BET, IR, UV–vis and ^{31}P NMR spectroscopies and thermal analysis (TG and DTA) and tested in methanol oxidation at 260 °C in the presence of molecular oxygen. The Dawson compounds were found to be active in this reaction and the product distribution (formaldehyde, methyl formate, dimethylether, dimethoxymethane) depends on the polyanion composition and on the framework symmetry. α-$K_6P_2W_{18}O_{62}$ exhibits an excellent catalytic performance with ca. 27% of methanol conversion and 98% of dimethylether selectivity. α1-$K_7P_2Mo_5VW_{12}O_{62}$ and α2-$K_7P_2Mo_5VW_{12}O_{62}$ show a similar activity (17–19% of conversion) with 49% of methyl formate selectivity and 41% of formaldehyde selectivity respectively. α-$K_6P_2Mo_6W_{12}O_{62}$ is the most oxidizing catalyst and the most selective toward the methyl formate (ca. 53%).

© 2011 Elsevier B.V. All rights reserved.

1. Introduction

The methanol oxidation is an attractive on-site source of H_2 for fuel cells [1–3] and can also lead to valuable oxygenated products such as formaldehyde (FA), methyl formate (MF), dimethyl ether (DME) and dimethoxymethane (DMM) which have various applications as solvent and/or precursor to many other chemical compounds. DME and DMM can also be used as oxygenated additives to fuel, owing to their high cetane number. In addition to these properties, DME, compound non-toxic, non-corrosive and biodegradable in air, can act as a clean fuel. The simplicity of this short carbon chain compound leads during combustion to very low emissions of particulate matter. Selective methanol oxidation to these different products was the subject of several studies. It has been reported that Sb—V mixed oxide [4] and supported rhenium oxide systems [5] are selective to formaldehyde, V_2O_5/TiO_2 [6], $H_{3+n}PMo_{12-n}V_nO_{40}$ Keggin [7] and Mn/Re/Cu catalysts [8] to dimethoxymethane and V—Ti—O materials [9] to methyl formate. On silica-supported 12-molybdophosphoric acid catalysts, it was shown that the distribution of reaction products depends on the loading and experimental conditions [10].

These works evidenced that methanol decomposition reaction is very sensitive to acidic and redox properties of solid and to experimental conditions. Thus, Tatibouët [11] showed that the decomposition of methanol could be used as a model reaction to characterize the acid–base and redox properties of a catalyst. The DME formation can describe the pure dehydration ability of a catalyst, which is generally related to its acidic character. The formation of DMM can be assigned to a dual site including a redox dehydrogenating site and a Lewis acid site, while the FA formation requires only a redox dehydrogenating site. Concerning, the MF and CO_2, their formation can be related to strong oxidative character of the catalyst.However, few works have tested the polyoxometallates (POMs) having the Dawson structure as catalysts compared to those of the Keggin structure. Dawson type compounds may be promising catalysts in homogeneous and heterogeneous systems because their redox and acidic properties can be controlled at atomic/molecular levels. They showed excellent catalytic activities in several reactions such as ethyl-tert-butyl ether [12], methyl tert-butyl ether [13] synthesis, both oxidative dehydrogenation of isobutyric acid [14] and isobutane [15] and hydroxylation of phenol [16].

The aim of this work was to prepare a series of Dawson-type POMs, as potassium salts, namely $K_6P_2Mo_xW_{18-x}O_{62}$ (x = 0, 5, 6) and α1 and α2-$K_7P_2Mo_5VW_{12}O_{62}$, in order to examine the effect of the chemical composition on their catalytic performance in methanol oxidation. POMs were characterized by BET, IR, UV–vis and ^{31}P NMR spectroscopies and thermal analysis (TG and DTA). The methanol conversion was carried out at 260 °C under atmospheric pressure in the presence of molecular oxygen.

* Corresponding author. Tel.: +213 21 24 73 11; fax: +213 21 24 73 11.
E-mail addresses: c_rabia@yahoo.fr, crabia@usthb.dz (C. Rabia).

1381-1169/$ – see front matter © 2011 Elsevier B.V. All rights reserved.
doi:10.1016/j.molcata.2011.12.024

2. Experimental

2.1. Materials

$K_6P_2W_{18}O_{62}$ was prepared according to the literature data [17]. Mixed W/Mo/V polyoxometallates $[P_2Mo_xV_yW_{18-(x+y)}O_{62}]^{n-}$ (x = 5, 6 and y = 0, 1) were obtained from the hexavacant anion $[H_2P_2W_{12}O_{56}]^{12-}$ according to the method described by Contant et al. [18] including the successive condensation and hydrolysis. $K_7P_2Mo_5VW_{12}O_{62}$ was obtained in the form of two α1 and α2 isomers. The different POMs were noted: α-P_2W_{18}, α2-$P_2Mo_5W_{13}$, α-$P_2Mo_6W_{12}$, α1-$P_2Mo_5VW_{12}$ and α2-$P_2Mo_5VW_{12}$.

2.2. Characterization

BET surface area measurements were performed at liquid nitrogen temperature using a Micrometrics ASAP 2020 V1.05 G apparatus. Prior to each adsorption–desorption measurement, the sample was degassed at T = 150 °C for 3 h. The specific surface areas were determined using the linear part of the BET equation.

Infrared spectra were recorded on the 4000–400 cm^{-1} range on a Bruker IFS 66 FT-IR spectrometer using samples prepared as KBr disks.

^{31}P MAS NMR spectra were measured at room temperature on a Bruker Avance 400 spectrometer. 85% H_3PO_4 was used as an external reference.

UV–vis diffuse reflectance spectra were recorded in the 800–200 nm region on a Varian Cary 5E spectrometer equipped with a polytetrafluoroethylene (PTFE) integration sphere. PTFE was used as a reference.

Thermogravimetric (TG) and differential thermal (DTA) data were collected on a SDT-2960 thermal analyzer. The TG and DTA experiments were performed under air flux, using 30 mg of sample and a heating rate of 1 °C/min.

2.3. Catalytic measurements

The methanol oxidation tests were carried out at 260 °C under atmospheric pressure using a Pyrex tubular flow micro reactor. A thermocouple was installed within the reactor, in contact with catalyst bed. The catalyst (20 mg) was first pretreated in situ for 1 h at 300 °C under an oxygen stream with a rate flow of 20 ml/min and then, the reactor was cooled down to the reaction temperature (260 °C). The flow of the initial reaction gas mixture (7.0 ml/min of N_2 and 1.5 ml of O_2) passed through a saturator filled with methanol at a partial pressure of 58.2 Torr. The flows of the initial reaction vapor–gas mixture and the final reaction mixture were connected in turn to the analyzer using the flow switcher. The analyzer is a gas-chromatographic (Cp-3800), instrument embedded in the system; it included a flame-ionization detector (FID) with a Carboxen 1000 column, a thermal-conductivity detector (TCD) with a chromosorb 107 column. The FID line allowed to analyze methanol, methyl formate (MF), formaldehyde (FA), dimethyl ether (DME) and dimethoxymethane (DMM) and the TCD line carbon monoxide (CO) and carbon dioxide (CO_2) noted CO_x.

3. Results

3.1. Characterization

The specific surface areas of Dawson POMs are very low (1–2 m^2/g) and similar to that of the Dawson heteropolyacid, $H_6P_2W_{18}O_{62}$ [19].

Fig. 1 shows the IR spectra of α-P_2W_{18}, $P_2Mo_6W_{12}$ and α1-$P_2Mo_5VW_{12}$. $[P_2W_{18}O_{62}]^{6-}$ Dawson heteropolyanion, constituted of two $[PW_9O_{31}]^{3-}$ units corresponding to the lacunary Keggin

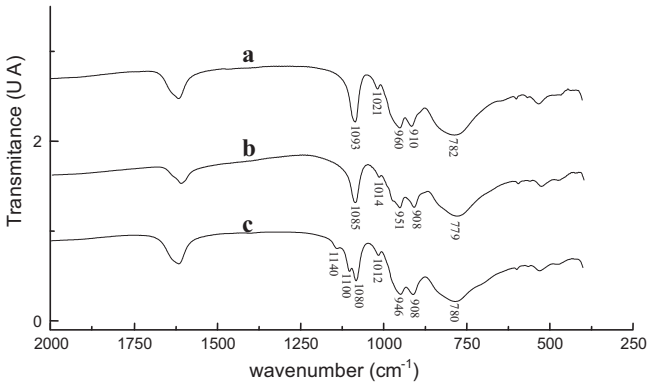

Fig. 1. IR Spectra of α-P_2W_{18} (a), α-$P_2Mo_6W_{12}$ (b) and α1-$P_2Mo_5VW_{12}$ (c).

anion, has been identified by four characteristic IR bands in the 1100–770 cm^{-1} range [20]. In addition to these vibration bands, several shoulders or small bands are observed for substituted heteropolyanions. The P—O band appears in the 1084–1100 cm^{-1} range while the M=O_d band appears in the 970–945 cm^{-1} range. The inter group M—O_b—M and the intra-group M—O_c—M bands appear around 910–908 cm^{-1} and 782–779 cm^{-1}, respectively. In addition of these four IR bands, another band is observed around 530 cm^{-1} corresponding to δ(P—O) vibration. The replacement of W atoms by Mo atoms only does not seem to have an effect on the IR vibration bands of Dawson polyanion, while an important perturbation is observed when vanadium is introduced into the Dawson unit. As shown on the IR spectrum of α1-$P_2Mo_5VW_{12}$ (Fig. 1c), two shoulders appear at 1140 and 1100 cm^{-1} on the P—O vibration band and one at 1012 cm^{-1} on the M=O_d vibration band.

In ^{31}P NMR spectroscopy, the chemical shift values depend on the composition and on the relative positions of the W, Mo and V atoms in the polyanion framework (Table 1). As already reported by Contant et al. [18], when the two half-anions are identical, the symmetric species show one signal, and when the species are unsymmetrical, two signals are observed. For α-P_2W_{18} and α-$P_2Mo_6W_{12}$, only one ^{31}P line is observed at −12.51 and −9.51 ppm, respectively in agreement with the equivalence of the two half-anions $[PW_9O_{31}]^{3-}$ and $[PW_6Mo_3O_{31}]^{3-}$, respectively. While $P_2Mo_5W_{12}$, α1-$P_2Mo_5VW_{12}$, and α2-$P_2Mo_5VW_{12}$ species gave two peaks at −9.39 and −10.08 ppm, at −9.73 and −10.10 ppm and at −8.95 and −9.76 ppm, respectively, in agreement with the lower symmetry of these polyanions due to two unequivalent half units.

Fig. 2 shows the polyhedral representation of the Dawson polyanion structure $[P_2W_{18}O_{62}]^{6-}$ and numbering of the metallic atoms according to IUPAC recommendations. In Dawson heteropolyanions, two different types of clusters are present: two terminal trimetallic groups M_3O_{13} (numbers 1–3 and 16–18) and six dimetallic groups M_2O_{10} (numbers 4–15) arranged in a double crown. The overall framework having a D_{3h} symmetry corresponds to α isomer. Mo_3O_{13} and Mo_2O_{10} clusters are connected to each other only by single μ-oxo-bridges and the local symmetry of all W(VI), Mo(VI) and V(V) is octahedral.Based on the results of tungsten, vanadium and phosphorus NMR spectroscopy, Contant et al. [18] assigned and marked the positions of molybdenum and vanadium atoms in the mixed W/Mo/V Dawson heteropolyanions as follows: 1,4,9,10,15,16-$P_2Mo_6W_{12}$; 1,9,10,15,16-$P_2Mo_5W_{13}$; 1,9,10,15,16-4-$P_2Mo_5VW_{12}$ (α1-$P_2Mo_5VW_{12}$) and 4,9,10,15,16-1-$P_2Mo_5VW_{12}$ (α2-$P_2Mo_5VW_{12}$).

UV–vis/diffuse reflectance spectroscopy (Fig. 3) shows that Dawson heteropolyanions exhibit strong absorption in the 650–200 nm wavelengths domain with multiplicity associated to ligand–metal charge transfers (LMCT) from oxygen to W(VI),

Table 1
^{31}P NMR chemical shifts and numbering of the metallic atoms according to the IUPAC for Dawson POMs.

POMs	Notation	δ (ppm)			
		P1	P2	Δδexp	Δδ [19]
$K_6[P_2W_{18}O_{62}]$	α-P_2W_{18}	−12.51	−2.51	0	0
1,4,9,10,15,16-$K_6[P_2Mo_6W_{12}O_{62}]$	α-$P_2Mo_6W_{12}$	−9.51	−9.51	0	0
1,4,9,10,15-$K_6[P_2Mo_5W_{13}O_{62}]$	α2-$P_2Mo_5W_{13}$	−9.39	−0.08	0.69	0.72
1,9,10,15,16-4-K_7 $[P_2Mo_5VW_{12}O_{62}]$	α1-$P_2Mo_5VW_{12}$	−9.73	−0.10	0.37	0.28
4,9,10,15,16-1-K_7 $[P_2Mo_5VW_{12}O_{62}]$	α2-$P_2Mo_5VW_{12}$	−8.95	−9.76	0.81	0.98

Δδexp = δ P1 − δ P2.

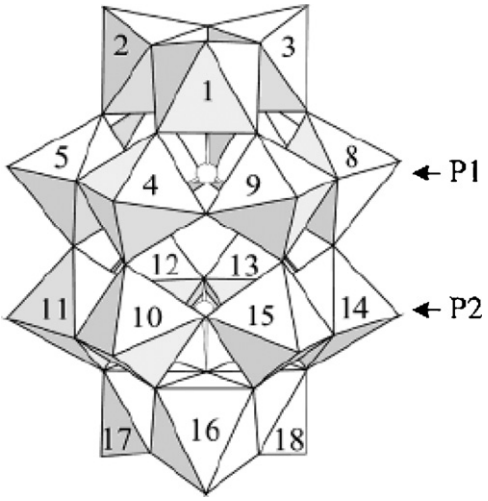

Fig. 2. Polyhedral representation of the Dawson structure of $[P_2W_{18}O_{62}]^{6-}$ polyanion.

Mo(VI) and V(V) in the Dawson anion. The position of the bands around 255 and 275 nm is attributed to M—O—M bridges (M: W, Mo and V) and the lowest energy absorption band shifts toward higher wavelength (from 350 to 420 nm) and broadens is related to size of the counter-ion. Similar results were obtained by other authors [21–25] which suggested that the presence of more than one band in the UV–vis spectra of Keggin-type or Dawson-type compounds results of the effect of several parameters such as the presence of different oxygen atoms (O_a, O_b, O_C and O_d), local symmetry, overall symmetry, polarizing and size of the counter-cation. An increase of cluster size or an increase of the polarizing effect and/or a decrease of the size of the counter-cation lead to a broadening and a red shift of the absorption band. It has also been reported that the broadening of the band can be assigned to the existence of interactions between polyanions.

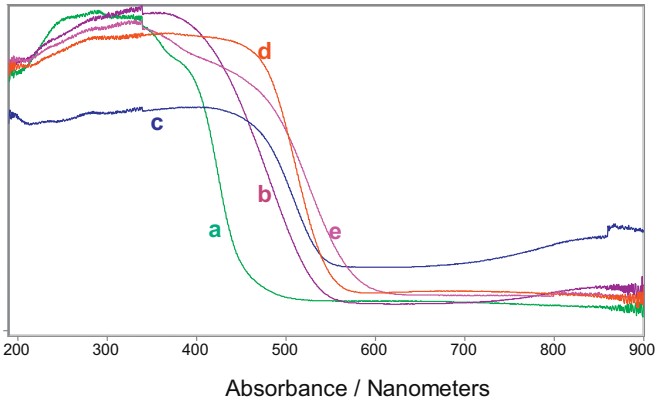

Fig. 3. UV–vis DR spectra of α-P_2W_{18} (a), α2-$P_2Mo_5W_{13}$ (b), α-$P_2Mo_6W_{12}$(c), α2-$P_2Mo_5VW_{12}$ (d) and α1-$P_2Mo_5VW_{12}$(e).

The width of the absorption band varies as follows: α2-$P_2Mo_5VW_{12}$ > α1-$P_2Mo_5VW_{12}$ > $P_2Mo_6W_{12}$ > $P_2Mo_5W_{13}$ > P_2W_{18}. The introduction of vanadium into the POM framework increases the negative charge of the polyanion, therefore the size of the cluster increases with the number of potassium atoms. This result is in agreement with literature data [24].

The thermal stability of the POMs was investigated by means of thermogravimetric (TG) and differential thermal analysis (DTA). The TG curve of P_2W_{18} (Fig. 4) shows a very low weight loss (∼1%) below 200 °C, attributed to the release of physisorbed water and between 200 and 500 °C, no other weight loss was observed. On the DTA diagram, two endothermic peaks are observed with maximum at 61 and 105 °C, associated to the mass loss observed in TG. No exothermal signal assigned to the POM decomposition is observed, suggesting that until 500 °C, the P_2W_{18} salt is stable.

The TG curves of $P_2Mo_5W_{13}$ and P_2 Mo_6W_{12} salts (Fig. 5) are similar to that of P_2W_{18} with also a low weight-loss (∼1%) below 200 °C. The DTA curves show three endothermic peaks at ca. 64, 100 and 140 °C in the case of $P_2Mo_5W_{13}$ and two endothermic peaks at ca. 110 and 140 °C in the case of $P_2Mo_6W_{12}$, associated also to the water mass loss. Small exothermal signal is observed at ca. 240 °C in presence of $P_2Mo_6W_{12}$ that could result from a change of isomeric form. The decomposition of both salts takes place at the same temperature (490 °C) indicating that the replacement of W atoms of P_2W_{18} Dawson unit by Mo atoms decreases the thermal stability of solid.

The DTA diagrams of α1 and α2-$P_2Mo_5VW_{12}$ (Fig. 5) show one broad endothermic peak with maximum at 86 and 78 °C respectively, associated to the release of physisorbed water, a wide exothermal signal assigned to α1 and α2-$P_2Mo_5VW_{12}$ decomposition with maximum at 430 and 450 °C, respectively. In the case of α1-$P_2Mo_5VW_{12}$, another small exothermic peak resulting probably from the exothermic crystallization of P_2O_5, WO_3, MoO_3 and V_2O_5 oxides is observed at ca. 460 °C. In the TG diagrams of these salts, only a continuous weight loss (∼2%), taking place mainly below 200 °C is observed. α2-$P_2Mo_5VW_{12}$ seems slightly more stable than α1-$P_2Mo_5VW_{12}$.

According to the DTA data, the thermal stability of Dawson POMs decreases as follows: $P_2W_{18} \gg P_2Mo_5W_{13} \approx P_2Mo_6W_{12}$ > α2-$P_2Mo_5VW_{12}$ > α1-$P_2Mo_5VW_{12}$. More W atoms are substituted

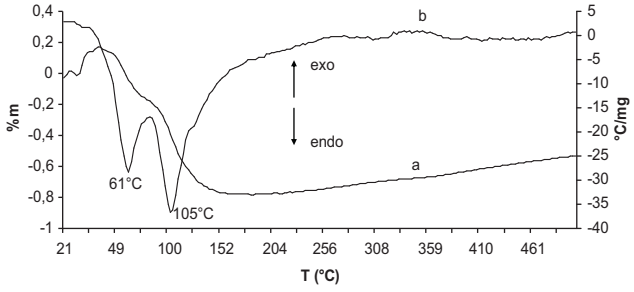

Fig. 4. TGA (a) and DTA (b) diagrams of α-P_2W_{18}.

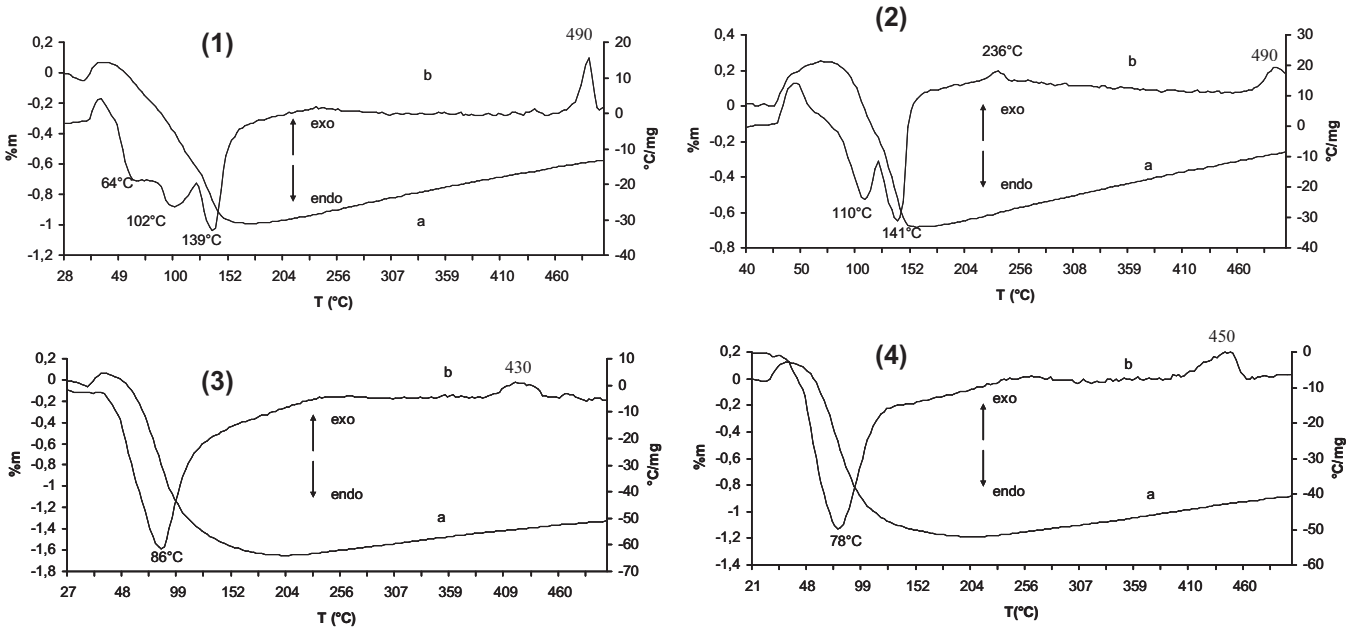

Fig. 5. TGA (a) and DTA (b) diagrams of α2-$P_2Mo_5W_{13}$ (1), α-$P_2Mo_6W_{12}$ (2), α1-$P_2Mo_5VW_{12}$ (3) and α2-$P_2Mo_5VW_{12}$ (4).

more the thermal stability is reduced, results in agreement with the lower symmetry of the polyanion.

Table 2 shows the IR bands frequencies of POMs after treatment at 300 °C for 1 h under oxidizing atmosphere (conditions of catalytic tests). No major modifications of frequencies of IR bands typical of the Dawson polyanion: υ_s(P—O_a) (1093–1081 cm^{-1}), υ_{as}(P—O_a) (1021–1015 cm^{-1}), ν_{as}(M=O_d) (976–948 cm^{-1}) ν_{as}(M—O_b—M) (916–881 cm^{-1}) and ν_s(M—O_c—M) (791–780 cm^{-1}), are observed for W/Mo and α2-$P_2Mo_5VW_{12}$, excepted for α1-$P_2Mo_5VW_{12}$ where the shoulder at 1102 cm^{-1} disappeared and the υ_s(P—O_a) shifted from 1082 to 1076 cm^{-1} indicating that α1-$P_2Mo_5VW_{12}$ solid is more sensitive to thermal pretreatment in agreement with DTA data. This study shows that the Dawson structure remains intact and that the substitution of W atoms by Mo and V atoms does not modify the stability of the polyanion framework during pretreatment of the solid.

These results are confirmed by those of the UV–vis study (Fig. 6), in which no major modification of the absorption band was observed after thermal treatment under (300 °C/O_2/1 h).The whole results on the thermal behavior of Dawson compounds showed that the structure of the polyanion was preserved under the conditions of catalytic test.

3.2. Catalytic tests

The catalytic properties of $K_6P_2Mo_xW_{18-x}O_{62}$ (x = 0, 5, 6) and α1 and α2-$K_7P_2Mo_5VW_{12}O_{62}$ Dawson type salts were examined in methanol oxidation by molecular oxygen at 260 °C after pretreatment in situ for 1 h at 300 °C under an oxygen stream. The Dawson compounds are active and the major products detected are formaldehyde (FA), methyl formate (MF), dimethylether (DME), and dimethoxymethane (DMM) and carbon oxides (noted CO_x) rather minor products.

Figs. 7–9 show the variations of the activity and the selectivities as a function of time for P_2W_{18}, $P_2Mo_5W_{13}$ and α1-$P_2Mo_5VW_{12}$.

No significant variation of both catalytic activity and DME selectivity was observed during more than 3 h of reaction in presence of P_2W_{18} (Fig. 7) suggesting a very good catalytic stability of this catalyst. This result is expected *to have working at low temperature (260 °C) and also* since Shikata et al. [13,19] showed that the reaction takes place in the solid bulk without the structure of the polyanion is modified. On the other hand, the study of the stability of α1-$K_xP_2Mo_{17}MO_{40}$ examined by IR, XRD, and by solution 31P NMR, after the isobutane oxydehydrogenation reaction at 450° during 100 h, showed that the catalyst was stable [15].

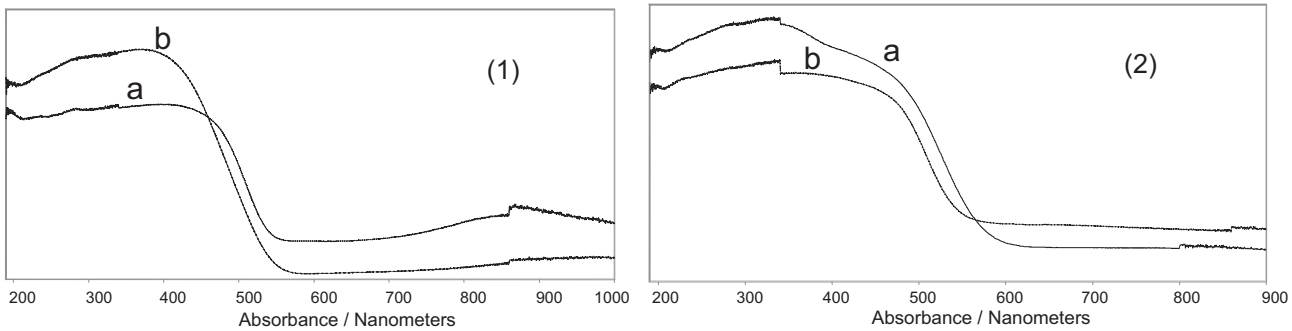

Fig. 6. UV–vis spectra of α-$P_2Mo_6W_{12}$ (1), α1-$P_2Mo_5VW_{12}$ (2), before (a) and after (b) thermal treatment (300 °C/1 h/O_2).

Table 2
FT-IR results of Dawson POMs before (a) and after (b) thermal treatment at 300 °C/1 h/O_2.

	IR frequencies (cm^{-1})				
	υ_s(P—O_a)	υ_{as}(P—O_a)	ν_{as}(M=O_d)	ν_{as}(M—O_b—M)	ν_s(M—O_c—M)
α-P_2W_{18} **(a)**	1093	1021	960	910	782
α-P_2W_{18} **(b)**	1090	1021	961	912	783
α-$P_2Mo_6W_{12}$ **(a)**	1089	1017	954	910	780
α-$P_2Mo_6W_{12}$ **(b)**	1081	1016	956	906	791
α1-$P_2Mo_5VW_{12}$ **(a)**	1102–1082	1015	948	911	785
α1-$P_2Mo_5VW_{12}$ **(b)**	1076	1015	976	881	788
α2-$P_2Mo_5VW_{12}$ **(a)**	1085	1016	948	916	786
α2-$P_2Mo_5VW_{12}$ **(b)**	1083	1015	945	915	787

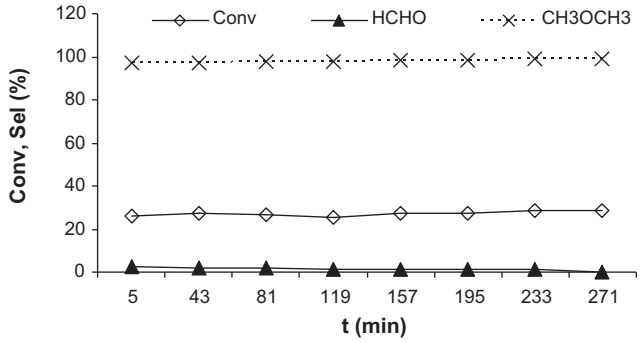

Fig. 7. Methanol conversion and product selectivities as a function of reaction time at 260 °C on α-P_2W_{18}, pretreated at 300 °C/1 h/O_2.

For α1-$P_2Mo_5VW_{12}$ (Fig. 8), the catalytic activity and the formation of products vary slowly with time-on-stream. Among the methanol oxidation products, MF seems to be the most stable. While in presence of $P_2Mo_5W_{13}$ catalyst, the variations of the catalytic activity and selectivities of different reaction products are more pronounced with time (Fig. 9). The methanol conversion increases gradually from 20 to 32% after more than 3 h of test. The selectivity toward DMM strongly increases with time from ca. 10% to ca. 35%, while that of FA decreases from ca. 35% to ca. 25%. This decrease can be attributed to the condensation reaction between methanol absorbed and FA to give DMM. The formation of the other reaction products is relatively stable during the catalytic test with MF and DME selectivities of ca. 20% and ca. 25–32%, respectively.

Table 3 shows the catalytic test results of $K_6P_2W_{18-x}Mo_x$ (x = 0, 5, 6) and α1 and α2-$K_7P_2Mo_5VW_{12}$ systems in methanol selective oxidation, obtained after around 3 h, when nearly steady-states were reached.

The catalytic activities of $P_2Mo_5W_{13}$ and P_2W_{18} are similar with 27.0 and 27.7% of conversion, higher than those of α1-$P_2Mo_5VW_{12}$ (18.7%) and α2-$P_2Mo_5VW_{12}$ (17.3%). $P_2Mo_6W_{12}$ seems to be the less active with only 11.8% of conversion. Contrary to the catalytic activity, product distribution is much more sensitive to both position and nature of transition metal in the framework. P_2W_{18} catalyst exhibits excellent catalytic performance in methanol oxidation with 98% of DME selectivity and 27% of conversion. The DME production by a bimolecular dehydration of methanol reflects the dehydration ability of a catalyst, generally related to its Brönsted or Lewis acidic character [8,11,13,16,19]. This result indicates that P_2W_{18} heteroplysalt have a strong acidic character of Lewis type assigned to high charge of W (VI). The dehydration of methanol has already observed on metal oxides as Mo/Al_2O_3 where only dimethyl ether was obtained as reaction product. The authors have attributed the Lewis acidic character of the catalyst to Mo(VI) and Al (III) [26].

The substitution of 5 W atoms by 5 Mo atoms led to a stronger decrease of the DME selectivity from ca. 98 to ca. 19% indicating a strong decrease of the acidic strength of the catalyst at the detriment of oxidative power. It is reported that the dimethyl ether formation can be considered as a parallel pathway of the methanol transformation which is controlled only by surface acidity [11]. It has been observed that the disappearance of the acidity of both SiO_2 supported $H_3PMo_{12}O_{40}$ [10] and SiO_2 supported $HMgPMo_{12}O_{40}$ [27] catalysts, pretreated at different temperatures, leads to a dramatic decrease in the rate of dimethyl ether formation to the benefit of that of redox products formed on oxidative centers. Thus, the presence of molybdenum favored the formation of oxidation products such as FA and MF with 27 and 28% of selectivity, respectively. DMM is obtained with ca. 25% of selectivity. These results indicate that $P_2Mo_5W_{13}$ catalyst presents both Lewis acid sites and oxidative sites with similar strengths.

The substitution of another W atom by one Mo atom in the $P_2Mo_5W_{13}$ system returns the methanol oxidation more selective to MF (ca. 53% of selectivity) and more selective to deep oxidation product (ca. 5% of carbon oxides selectivity). The other reaction products are FA and DME with ca. 18 and ca. 23% of selectivity,

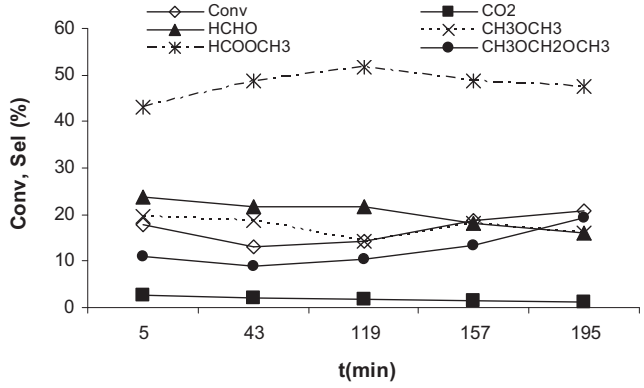

Fig. 8. Methanol conversion and product selectivities as a function of reaction time at 260 °C on α1-$P_2Mo_5VW_{12}$, pretreated at 300 °C/1 h/O_2.

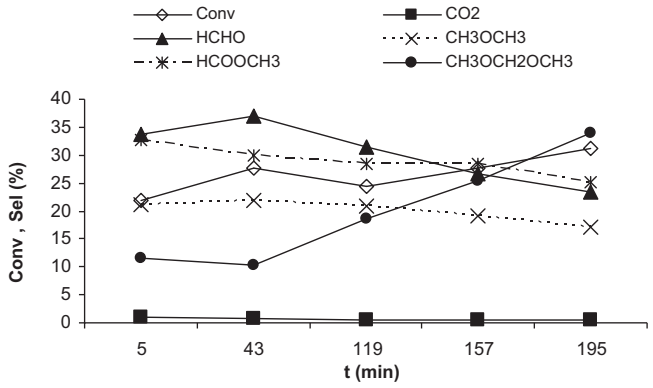

Fig. 9. Methanol conversion and product selectivities as a function of reaction time at 260 °C on α2-$P_2Mo_5W_{13}$, pretreated at 300 °C/1 h/O_2.

Table 3
Catalytic performance of Dawson POMs, pretreated at 300 °C/2 h/O_2, for the methanol oxidation at 260 °C.

%	POMs				
	α-P_2W_{18}	α2-$P_2Mo_5W_{13}$	α-$P_2Mo_6W_{12}$	α1-$P_2Mo_5VW_{12}$	α2-$P_2Mo_5VW_{12}$
Conv	27.3	27.7	11.8	18.7	17.3
CO_2	0.0	0.4	4.7	1.4	2.9
HCHO	1.3	26.6	18.4	18.2	40.8
CH_3OCH_3	98.4	19.2	23.4	18.2	26.4
HCO_2CH_3	0.0	28.4	53.4	48.8	18.9
$(CH_3O)_2CH_2$	0.0	25.3	0.0	13.3	11.0

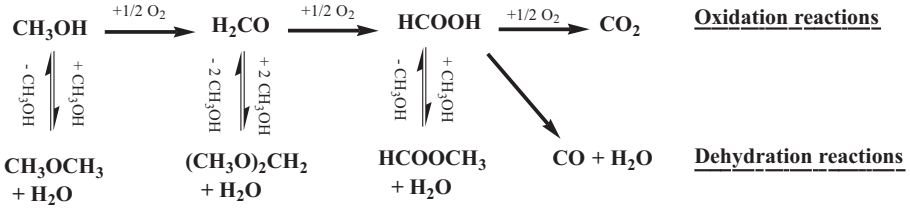

Scheme 1. Reaction pathways in methanol conversion [11].

respectively. DMM product has not been observed. With respect to the position of Mo atoms in the polyanion structure (1,4,9,10,15,16-$P_2Mo_6W_{12}$), the methanol oxidation to MF, FA and CO_x (sum of selectivities = 76%) over this catalyst, could occur on the polyanion face that could correspond to a concentration of oxidative active sites related to Mo=O and Mo—O—Mo bonds. Thus, $P_2Mo_6W_{12}$ presents a very strong oxidative character compared to $P_2Mo_5W_{13}$, but also an acidic character with a moderate strength.

In P/W/Mo/V systems, the vanadium position in framework polyanion have an important effect on the product distribution and therefore on acid and redox properties of the catalyst. Thus, α1-$P_2Mo_5VW_{12}$ (1,9,10,15,16-4-$P_2Mo_5VW_{12}$), with the vanadium atom, in position 4 in a dimetallic group M_2O_{10} cluster, is selective to MF with ca. 50% of selectivity. FA and DME are obtained with similar selectivity of ca. 18% higher than that of DMM (ca. 13%). While α2-$P_2Mo_5VW_{12}$ (4,9,10,15,16-1-$P_2Mo_5VW_{12}$) with the vanadium atom, in position 1 in a trimetallic group M_3O_{13} cluster, is selective toward FA with ca. 41% of selectivity. MF, DME and DMM are obtained with selectivities of ca. 19, 26 and 11%, respectively. These results show that both catalysts exhibit a good synergistic effect of the reducibility and acidic property in the methanol oxidation with a moderate relative acidic density and a high oxidative power. However, when the vanadium atom is in position 4, the catalyst seems to be more oxidative (sum of FA, MF, CO_x selectivities: ca. 67 against 63%). In position 4, the active sites are probably V=O and/or Mo—O—V, more oxidizing sites and in position 1, W—O—V and/or Mo—O—V.

From the catalytic properties of Dawson-type POMs in the methanol oxidation reaction, the oxidative power of the substituted POMs decreases in the following order: α-$P_2Mo_6W_{12}$ > α1-$P_2Mo_5VW_{12}$ > α2-$P_2Mo_5VW_{12}$ ≫ α2-$P_2Mo_5W_{13}$. P_2W_{18} presents only an acidic character.

The DME formation reflecting the acidic character of catalyst is related to the presence of W atoms. The acidic character increases with W atom number. The efficiency of P_2W_{18}, in its acid form has already been reported by Misono et al. [13,19] in the gas phase synthesis of methyl tert-butyl ether from methanol. The authors showed that the catalytic activity of P_2W_{18} heteropolyacid for this reaction was at least 13 times greater than that of Keggin type HPAs ($H_nXW_{12}O_{40}$, X = P, Si, Ge, B, and Co). From this result, the authors suggested that the activity of catalyst was not governed only by both acid strength and surface area of $H_6P_2W_{18}O_{60}$ which are lower than those of parent Keggin type heteropolyacids, $H_3PW_{12}O_{40}$ and $H_4SiW_{12}0_{40}$, but by another property lied to the presence of the pseudoliquid phase. It is generally accepted in acid catalysis, that the reaction takes place in the bulk of the polyoxometallate, assimilated to a pseudoliquid phase, where the solid catalyst behaving in a sense like a concentrated solution. Thus, the bulk phase is the reaction field. The high-activity state of the pseudoliquid phase and the rapid absorption–desorption of reactive and products are probably the reasons for the high activity of P_2W_{18}. Moreover, this performance can be related to the shape of Dawson-type heteropolyanion which is not spherical as that of Keggin-type and that the secondary structure of Dawson polyoxometallate may be less ordered and less rigid.

FA formation that requires only a redox dehydrogenating site is observed after introduction of Mo and V atoms. Its selectivity is particularly high when the V atom is in position 1 in the trimetallic group cluster. The oxidative power introduced by Mo and V atoms has already been observed in the case of both Keggin and Dawson type heteropolyanions [7,14]. The redox sites were attributed to the metal-terminal oxygen bond (M=Od).

DMM formation can be assigned to the condensation reaction between methanol, rapidly absorbed into the pseudoliquid phase and the formed product (FA) and MF formation can be assigned to an esterification reaction between methanol and formic acid which would come from the FA oxidation. The presence of the formic acid considered as an intermediate in the formation of MF, has not been reported in the literature works. The products, DMM and MF, require both redox sites and acid sites. The redox sites are in charge of transferring the lattice oxygen to adsorbed methanol to form formaldehyde and formic acid, while the acid sites catalyze the condensation of the intermediates with methanol to form DMM and MF [28]. These different reactions may occur at the surface and solid bulk of the polyanions as shown the scheme de reaction pathways (Scheme 1) suggested by Tatibouët [11], where the oxidation of methanol involves several sequential and parallel reactions.

This study evidenced the high sensitivity of methanol oxidation to both composition and relative positions of the W, Mo, and V atoms in the framework of Dawson polyanion. These two parameters lead to different acidic and redox properties that control the selectivity orientation between the formations of dehydration and/or redox products.

4. Conclusion

The Dawson type V-substituted molybdo-tungstodiphosphates, $K_6P_2Mo_xW_{18-x}O_{62}$ (x = 0, 5, 6) and α1 and

α2-$K_7P_2Mo_5VW_{12}O_{62}$, synthesized, characterized by different techniques (BET, IR, UV–vis and ^{31}P NMR spectroscopies) and thermal analysis (TG and DTA) and tested in a probe reaction such as methanol oxidation display a series of interesting properties in relation with the combination of various atomic compositions and the framework symmetry: (i) α-$K_6P_2W_{18}O_{62}$ very selective to dimethylether reflecting its high acidic character; (ii) α1-$K_7P_2Mo_5VW_{12}O_{62}$ selective methyl formate and α2-$K_7P_2Mo_5VW_{12}O_{62}$ to formaldehyde reflecting their bi-functional acid-oxidative character; (iii) α-$K_6P_2Mo_6W_{12}O_{62}$ very selective to methyl formate reflecting its high oxidative character.

This study showed that the composition and relative positions of the W, Mo, and V atoms in the framework of Dawson polyanion lead to different acidic and redox properties that control the selectivity orientation between the formations of dehydration and/or oxidation products. Thus, the Dawson POMs appear as a good design to direct the selective oxidation of methanol toward the desired products by the choice of elements constituting the heteropolyanion.

References

[1] R. Ubago-Perez, F. Carrasco-Marin, C. Moreno-Castilla, Catal. Today 123 (2007) 158–163.
[2] C. Cao, K.L. Hohn, Appl. Catal. A: Gen. 354 (2009) 26–32.
[3] Z. Wang, W. Wang, G. Lu, Int. J. Hydrogen Energy 28 (2003) 151–158.
[4] H. Zhang, Z. Liu, Z. Feng, C. Li, J. Catal. 260 (2008) 295–304.
[5] Y. Yuan, Y. Iwasawa, J. Phys. Chem. B 106 (2002) 4441–4449.
[6] Y. Fu, J. Shen, Chem. Commun. (2007) 2172–2174.
[7] H. Liu, E. Iglesia, J. Phys. Chem. B 107 (2003) 10840–10847.
[8] H. Li, J.P. Li, F.K. Xiao, W. Wei, Y.H. Sun, J. Fuel Chem. Technol. 37 (2009) 613–617.
[9] E. Tronconi, A.S. Elmi, N. Ferlazzo, P. Forzatti, Ind. Eng. Chem. Res. 26 (1987) 1269–1275.
[10] C. Rocchiccioli-Deltcheff, A. Aouissi, S. Launay, M. Fournier, J. Mol. Catal. A: Chem. 114 (1996) 33l–342l.
[11] J.M. Tatibouët, Appl. Catal. A 148 (1997) 213–252.
[12] J. Pozniczek, A. Lubanska, D. Micek-Ilnicka, E. Mucha, A. Lalik, A. Bielanski, Appl. Catal. A: Gen. 298 (2006) 217–224.
[13] S. Shikata, S. Nakata, T. Okuhara, M. Misono, J. Catal. 166 (1997) 263–271.
[14] D.R. Park, H. Kim, J.C. Jung, S.H. Lee, I.K. Song, Catal. Commun. 9 (2008) 293–298.
[15] F. Cavani, R. Mezzogori, A. Trovarelli, J. Mol. Catal. A 204–205 (2003) 599–607.
[16] J. Yu, P. Yang, Y. Yang, T. Wu, Catal. Commun. 7 (2006) 153–156.
[17] J. Randall, D.K. Lyon, R.J. Domaille, R.G. Finke, A.P. Ginsberg, A Wiley-Interscience Publication, John Wiley and Sons, New York, Chichester, Brisbane, Toronto, Singapore, 1998.
[18] R. Contant, M. Abbessi, R. Thouvenot, G. Hervé, Inorg. Chem. 43 (2004) 3597–3604.
[19] S. Shikata, T. Okuhara, M. Misono, J. Mol. Catal. A: Chem. 100 (1996) 49–59.
[20] C. Rocchiccioli-Deltcheff, Spectrosc. Lett. 12 (2) (1979) 127–138.
[21] F. Cavani, R. Mezzogori, A. Pigamo, F. Trifiro, Chem. Eng. J. 82 (2001) 33–42.
[22] T. Mazari, C. Marchal-Roch, S. Hocine, N. Salhi, C. Rabia, J. Nat. Gas Chem. 18 (2009) 319–324.
[23] L. Dermeche, R. Thouvenot, S. Hocine, C. Rabia, Inorg. Chim. Acta 362 (2009) 3896–3900.
[24] T. Mazari, C. Marchal-Roch, S. Hocine, N. Salhi, C. Rabia, J. Nat. Gas Chem. 19 (2010) 54–60.
[25] M. Fournier, C. Louis, M. Che, P. Chaquin, D. Masures, J. Catal. 119 (1989) 400–414.
[26] M. Brandhorst, S. Cristol, M. Capron, C. Dujardin, H. Vezin, G. Le bourdon, E. Payen, Catal. Today 113 (2006) 34–39.
[27] J.M. Tatibouët, C. Montalescot, K. Brücknan, J. Haber, M. Che, J. Catal. 169 (1997) 22–32.
[28] E. ÉcouteLire phonétiquemTronconi, A.S. Elmi, N. Ferlazzo, P. Forzatti, Ind. Eng. Chem. Res. 26 (1987) 1269–1275.